Intermetallic Phases

DOI: 10.1002/anie.201309723

Building Nanocomposite Magnets by Coating a Hard Magnetic Core with a Soft Magnetic Shell**

Fei Liu, Jinghan Zhu, Wenlong Yang, Yunhe Dong, Yanglong Hou, Chenzhen Zhang, Han Yin, and Shouheng Sun**

Abstract: *Controlling exchange coupling between hard magnetic and soft magnetic phases is the key to the fabrication of advanced magnets with tunable magnetism and high energy density. Using FePt as an example, control over the magnetism in exchange-coupled nanocomposites of hard magnetic face-centered tetragonal (fct) FePt and soft magnetic Co (or Ni, Fe_2C) is shown. The dispersible hard magnetic fct-FePt nanoparticles are first prepared with their coercivity (H_c) reaching 33 kOe. Then core/shell fct-FePt/Co (or Ni, Fe_2C) nanoparticles are synthesized by reductive thermal decomposition of the proper metal precursors in the presence of fct-FePt nanoparticles. These core/shell nanoparticles are strongly coupled by exchange interactions and their magnetic properties can be rationally tuned by the shell thickness of the soft phase. This work provides an ideal model system for the study of exchange coupling at the nanoscale, which will be essential for building superstrong magnets for various permanent magnet applications in the future.*

Nanocomposite magnets containing hard magnetic and soft magnetic phases are believed to be essential to build superstrong magnets for clean energy and other magnetic applications.[1] In the nanocomposite structure, the soft phase needs to couple strongly with the hard phase so that its magnetization direction can rotate coherently with that of the hard phase.[2] To realize efficient exchange coupling, the soft phase should have a size of about twice the domain wall width of the hard phase, which is often in the nanometer scale.[3,4] A strong exchange coupling can ensure the composite retaining large coercivity, H_c, from the hard phase with increased magnetization, M, from the soft phase. Such a nanocomposite magnet should have a large energy product and a high energy density. It also allows rational tuning of the nanocomposite composition, making it possible to understand multiphase magnetism at the nanoscale and to apply the optimal magnetic property for targeted magnetic applications.[5,6] The FePt alloy with a face-centered tetragonal (fct) structure has been the choice for the hard magnetic phase to study exchange coupling in nanocomposites because of their large magnetocrystalline anisotropy (K_U) and superior chemical stability.[7] However, the process leading to intimate contact between a soft phase, such as Fe or Co, and a hard FePt phase needs a high temperature, causing partial diffusion between the hard and soft phase elements.[8,9] As a result, it has been very challenging to prepare fct-FePt-based nanocomposites with a distinct soft phase present in the FePt matrix,[10–15] making it impossible to study the size effect of the soft phase on the magnetic performance of the nanocomposites.

Herein we report a general protocol for the synthesis of exchange-coupled nanocomposites with hard magnetic fct-FePt as the core and soft magnetic Co (or Ni, Fe_2C) as the shell and with their magnetic properties being tuned by the shell thickness. Previously, fct-FePt nanoparticles (NPs) were prepared by high-temperature annealing of face-centered cubic (fcc)-FePt NPs, after which the fct-FePt NPs were not dispersible in any solvent. Recently, dispersible fct-FePt NPs were prepared by annealing of fcc-FePt/Fe_3O_4/MgO at 650 °C in Ar containing 5 % H_2.[16] In this process, Fe_3O_4 coating was used to create void defects around FePt NPs upon reduction of Fe_3O_4 and to facilitate Fe and Pt diffusion into fct-FePt. MgO coating protected the diffusion and fct-formation processes and could be removed by washing with an acidic aqueous solution. But upon MgO removal, these fct-FePt NPs needed to be stabilized by oleic acid and hexadecanethiol and the strong thiol-Pt interaction made the fct-FePt inaccessible for further magnetic modifications. We noticed that the fct-FePt/MgO NPs could be dispersed in ethanol, allowing acid etching of MgO in ethanol, and more importantly, facilitating fct-FePt stabilization by oleic acid (OA) and oleylamine (OAm). These oleate/oleylamine-coated fct-FePt NPs could serve as seeds for Co (or Ni, Fe_2C) coating in a high-temperature solution-phase reduction process. These core/shell NPs show the desired exchange coupling and shell-thickness-dependent magnetic properties, providing an ideal model system for the study of exchange coupling at the nanoscale and for the fabrication of nanocomposite magnets with a high energy density.

To make fct-FePt NPs, we first prepared composite fcc-FePt-Fe_3O_4 NPs from a one-pot reaction of iron pentacarbonyl ($Fe(CO)_5$), platinum acetylacetonate ($Pt(acac)_2$), OA,

[*] F. Liu, J. Zhu, W. Yang, Y. Dong, Prof. Y. Hou, C. Zhang, H. Yin
Department of Materials Science and Engineering
College of Engineering, Peking University
Beijing 100871 (China)
E-mail: hou@pku.edu.cn
Prof. S. Sun
Department of Chemistry, Brown University
Providence, RI 02912 (USA)
E-mail: ssun@brown.edu

[**] This work was supported by the National Basic Research Program of China (grant number 2010CB934601), the NSFC (grant numbers 51125001, 51172005, and 90922033), the Natural Science Foundation of Beijing (grant number 2122022), Yok Ying Tung Found (grant number 122043), the Doctoral Program (grant number 20120001110078) and New Century Talent of the Education Ministry of China (grant number NCET-09-0177).

Supporting information for this article is available on the WWW under http://dx.doi.org/10.1002/anie.201309723.

and OAm in 1-octadecene, and coated these NPs with MgO by decomposition of magnesium(II) acetylacetonate hydrate ($Mg(acac)_2{\cdot}2H_2O$) in the presence of OA and OAm in benzyl ether at 300 °C. The synthesis of fcc-FePt-Fe_3O_4 NPs was similar to what has been reported,[16,17] but our MgO coating method was simplified further from what reported previously,[18] and no 1,2-tetradecanediol was used for MgO formation. The presence of an controlled amount of OAm and OA was the key to the MgO coating. The absence of OA would lead to a mixture of FePt-Fe_3O_4 and MgO NPs. When OAm/OA was in 3 to 30, MgO preferred to nucleate on the surface of FePt-Fe_3O_4 seeds. In the presence of a larger amount of OA (OAm/OA $\leq$1.5), the Mg complex was difficult to decompose into MgO. Figure 1 a/b shows the transmission electron microscopy (TEM) images of the as-synthesized FePt-Fe_3O_4 and FePt-Fe_3O_4/MgO NPs.

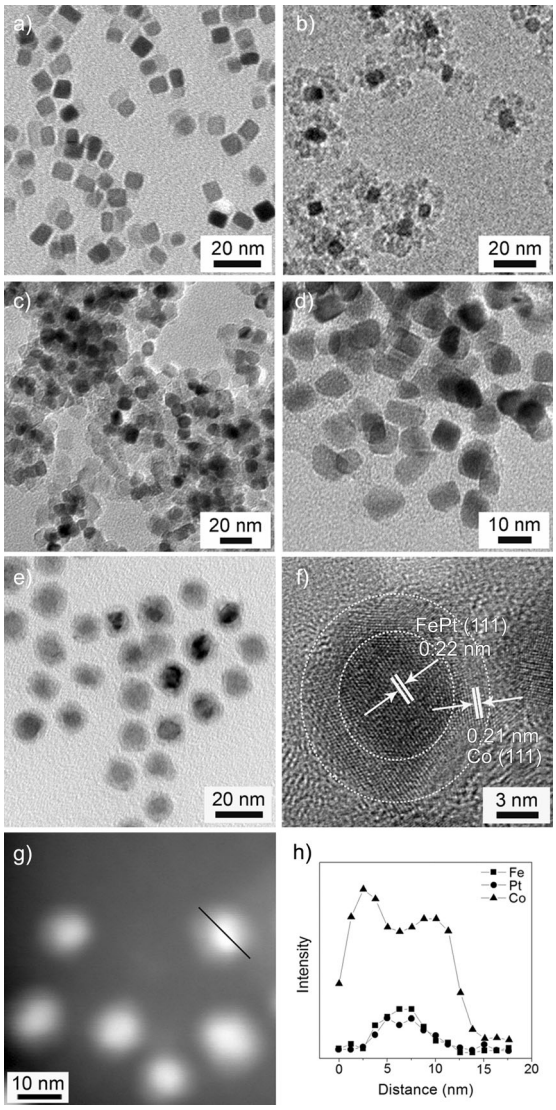

Figure 1. TEM images of the a) fcc-FePt-Fe_3O_4 NPs, b) fcc-FePt-Fe_3O_4/MgO NPs, c) fct-FePt/MgO NPs, d) fct-FePt NPs, and e) 8/4 nm FePt/Co core/shell NPs. f) HRTEM image of a 8/4 nm FePt/Co core/shell NP. g) HAADF-STEM image of the FePt/Co NPs, and h) EDS profile obtained by scanning a single FePt/Co NP illustrated in (g).

The fcc-FePt-Fe_3O_4/MgO NPs were converted into fct-FePt/MgO NPs by thermal annealing at 700 °C in Ar containing 5 % H_2. In this process, hydrogen reduces Fe_3O_4 to Fe, which further diffuses into FePt matrix to form fct-FePt. The X-ray diffraction (XRD) pattern (see Figure S1a in the Supporting Information) of the annealed FePt/MgO NPs shows the characteristic fct (001) and (110) peaks, indicating the formation of the fct structure. The TEM image (Figure 1 c) shows that the fct-FePt NPs (8 nm) are embedded in the MgO matrix without any sintering. These fct-FePt/MgO NPs could be dispersed in ethanol and the MgO shell was removed by adding several drops of the concentrated nitric acid into the ethanol dispersion. This acid treatment did not change the FePt structure and morphology as indicated by the XRD pattern (Figure S1b) and the TEM image (Figure 1 d).

The isolated fct-FePt NPs were collected from the ethanol dispersion by centrifugation and further transformed into hexane with the assistance of OA and OAm as surfactants. To prepare 8/4 nm FePt/Co NPs, the 8 nm fct-FePt NPs (8 mg) were dispersed in hexane (5 mL) and injected into the degassed solution containing $Co(acac)_2$ (40 mg) and OAm (10 mL) at 120 °C. After hexane was totally evaporated, the reaction mixture was heated up to 320 °C and maintained at this temperature for 1 h in Ar + 5 % H_2. The Co shell thickness was controlled by tuning the molar ratio between the seed and the precursor. For example, 160 mg $Co(acac)_2$ in the solution produced 8/6 nm FePt/Co NPs, while 320 mg $Co(acac)_2$ led to 8/9.5 nm FePt/Co NPs.

Figure 1 e shows the TEM image of the representative 8/4 nm FePt/Co core/shell NPs. TEM images of the NPs with thicker Co shells of 6 and 9.5 nm are presented in Figure S2a/b, respectively. Table S1 summarizes the dimensions and dimension distributions of the core and shell. Because of the difference in the electron scattering power of FePt and Co, the core/shell structure is easily seen with a dark core diameter of about 8 nm and a lighter shell thickness of about 4 nm. Figure 1 f displays a high-resolution TEM (HRTEM) image of a single 8/4 nm FePt/Co particle. The core lattice spacing is measured to be 0.22 nm, corresponding to the (111) plane of the fct-FePt. The shell lattice fringe distance is 0.21 nm from the (111) plane of fcc-Co. The high-angle annular dark-field scanning TEM (HAADF-STEM) image shown in Figure 1 g and the line elemental energy-dispersive spectroscopy (EDS) profile across the whole particle (Figure 1 h) further confirm the FePt/Co core/shell nanostructure.

Figure 2 shows the XRD patterns of the FePt/Co core/shell NPs with different shell thickness. The typical fct structure of FePt and the fcc structure of Co can be seen in each XRD pattern. As the Co thickness increases, the Co diffraction peak sharpens, indicating the presence of larger crystal Co domains in the core/shell structure. The electronic structure of Co in the shell was characterized by X-ray photoelectron spectroscopy (XPS). The peak at 778.1 eV in the Co2p spectrum (Figure S3) can be assigned to metallic Co. Furthermore, the peaks at about 780 and 797 eV are characteristic of CoO, suggesting the surface oxidation of the Co shell.

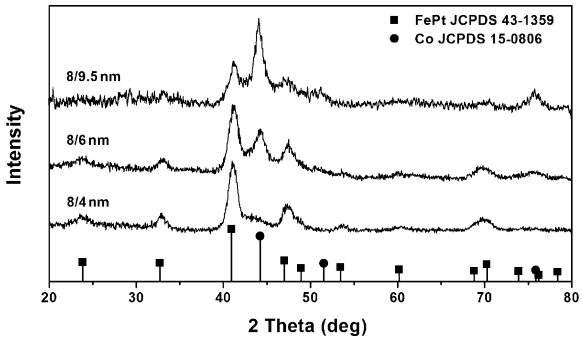

Figure 2. XRD patterns of the FePt/Co core/shell NPs with different Co shell thickness.

Room-temperature hysteresis loops of the as-synthesized 8 nm fct-FePt NPs and 8/4 nm fct-FePt/Co core/shell NPs are shown in Figure 3a. The fct-FePt NPs are ferromagnetic at room temperature with a large H_c of 33 kOe and a saturation magnetization (M_s) of 33 emu g^{-1}. For the FePt/Co core/shell NPs, the hysteresis loop behaves like a single magnetic phase, indicating the coherent magnetization rotation and good exchange coupling between fct-FePt and Co. Previous theoretical studies suggest that for the effective exchange coupling, the thickness of the soft phase needs to be twice the width of the domain wall δ_W of the hard phase.[3,4] For fct-FePt phases, the domain wall thickness δ_W calculated from $\delta_W = \pi(A/K_U)^{1/2}$, in which $A \approx 10^{-6}$ erg cm^{-1} for the exchange coupling constant and $K_U \approx 6.6 \times 10^7$ erg cm^{-3} for the uniaxial anisotropy constant, is estimated to be 4 nm.[19] The Co shell thickness (4 nm) in this study is well within the limit of $2\delta_W =$ 8 nm, hence Co and fct-FePt are effectively coupled by exchange interactions. For 8/4 nm FePt/Co core/shell NPs, the H_c decreases to a value of 8.4 kOe compared to that of the 8 nm fct-FePt NPs, while the M_s is increased to 54 emu g^{-1}. By adjusting the Co shell thickness, the magnetic properties of the FePt/Co core/shell NPs can be readily controlled. Figure 3b summarizes the Co shell-thickness-dependent M_s and H_c data for the FePt/Co NPs. A thicker Co shell leads to a smaller H_c and a higher M_s. In both cases, the soft and hard phases in the core/shell NPs are effectively coupled by exchange interactions.

The fct-FePt/Co core/shell NPs can be used as building blocks to fabricate exchange-coupled FePt/Co nanocomposites using a mild annealing process. Figure 3c shows the hysteresis loops of the samples from 8/4 nm FePt/Co NPs annealed at 300 and 350 °C in Ar containing 5 % H_2 for 1 h. The smooth magnetization transition observed from both samples infers the maintained exchange coupling in the nanocomposites. For the sample annealed at 300 °C, the values of M_s and H_c are 60 emu g^{-1} and 6.4 kOe, respectively. Compared to the untreated NPs, there is a drop in H_c and increase in M_s upon annealing. When the annealing temperature is increased to 350 °C, the H_c value of the nanocomposite further decreases to 4.7 kOe, while its M_s increases to 65 emu g^{-1}. The increased M_s can be ascribed to the reduction of CoO on the surface and the grain growth of Co. On the other hand, the interfacial diffusion between FePt and Co during the annealing process may contribute to the decreased H_c.[20] The magnetic properties of the fct-FePt/Co composites with different Co shell thickness were also studied. Figure 3d summarizes the Co shell-thickness-dependent M_s and H_c for the nanocomposites annealed at 300 °C. With the increased shell thickness, the H_c of the annealed samples decreases from 6.4 to 0.8 kOe while the M_s increases from 60 to 140 emu g^{-1}.

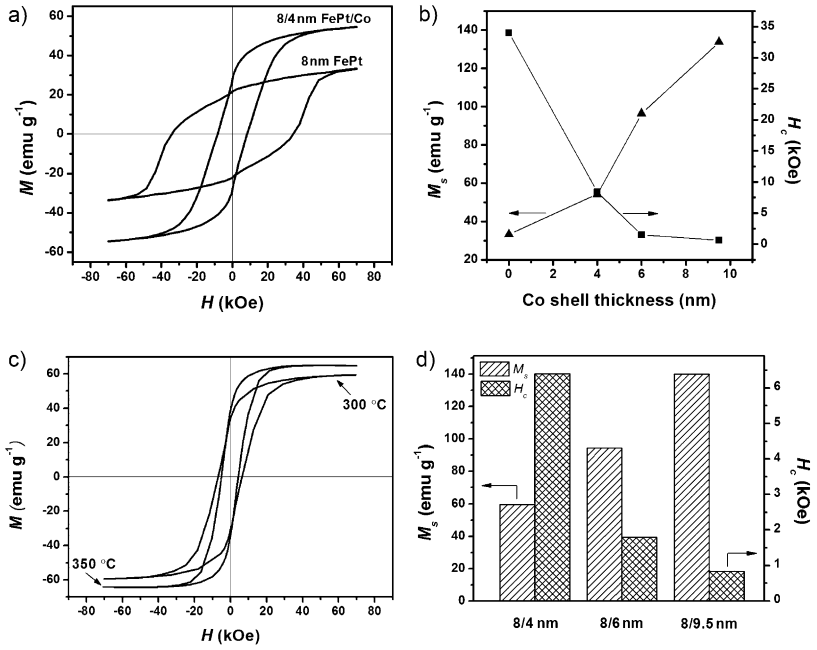

Figure 3. a) Room-temperature hysteresis loops of fct-FePt NPs and 8/4 nm FePt/Co core/shell NPs. b) Co shell-thickness-dependent M_s and H_c for the FePt/Co core/shell NPs. c) Room-temperature hysteresis loops of the FePt/Co nanocomposites annealed from 8/4 nm FePt/Co core/shell NPs at 300 and 350 °C. d) M_s and H_c of the FePt/Co nanocomposites annealed from FePt/Co core/shell NPs with different Co shell thickness.

This seed-mediated approach can be extended to synthesize other FePt-based core/shell NPs by simply altering the precursors used in the reaction. Using a similar procedure, FePt/Ni and FePt/Fe_2C core/shell NPs could be prepared (Table S1). Figure 4a is the TEM image of the 8/4 nm FePt/Ni NPs. The lattice spacing measured from the HRTEM image in Figure 4b implies that the FePt/Ni core/shell nanostructure possesses an interface which is between the (110) face of FePt and the (111) face of Ni. Figure S4a displays the TEM image of the 8/4 nm FePt/Fe_2C NPs. The core has an interplanar distance of 0.19 nm, corresponding to the (002) plane of fct-FePt (Figure S4b). The lattice spacing of 0.21 nm in the inner shell corresponds to the hexagonal Fe_2C (101) plane, and the lattice spacing of 0.25 nm for the outer shell can be assigned to the (311) plane of Fe_3O_4, which is attributed to the oxidation of Fe_2C. XRD patterns (Figure S5), XPS analyses (Figure S6), HAADF-STEM images (Fig-

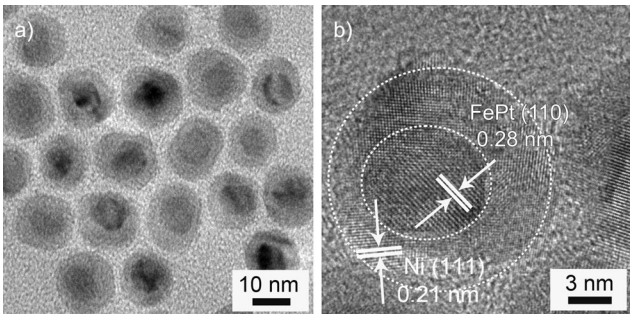

Figure 4. a) TEM and b) HRTEM images of the 8/4 nm FePt/Ni core/shell NPs.

ure S7a/c), and line elemental EDS data measured across the whole particle (Figure S7b/d) further confirm the FePt/Ni and FePt/Fe_2C core/shell nanostructures. Furthermore, the thickness of either the Ni or Fe_2C shell (Figure S8) and the core/shell magnetism (Figure S9) can be readily controlled by tuning the molar ratio between the seeds and precursors.

In conclusion, we have developed a general strategy to prepare exchange-coupled nanocomposites by coating the magnetic hard core of fct-FePt with a soft magnetic shell of Co (or Ni, Fe_2C). By reductive decomposition of $Co(acac)_2$ in the OAm solution in the presence of fct-FePt NPs, FePt/Co core/shell NPs with a Co shell thickness from 4 to 9.5 nm can be produced. The FePt/Co core/shell NPs are strongly exchange-coupled and their H_c are tunable from 33 (no Co shell) to 0.6 kOe (9.5 nm Co shell) while the M_s are controlled from 33 to 133 emu g^{-1}. The core/shell NPs can be used as building blocks to fabricate exchange-coupled FePt/Co nanocomposites with their magnetic properties readily tuned by the core/shell dimensions. Our synthesis is simple and has been extended to the preparation of FePt/Ni and FePt/Fe_2C core/shell NPs and nanocomposites. Using a similar synthetic strategy, we should be also able to prepare Fe- or FeCo-coated FePt NPs. These core/shell NP systems are ideal models for understanding exchange interactions at the nanoscale, which will be essential for building superstrong magnets for various permanent magnet applications in the future.

Experimental Section

Synthesis of FePt-Fe_3O_4 NPs: In a four-neck flask, a mixture of Pt^{II} acetylacetonate ($Pt(acac)_2$, 0.1 g, 0.25 mmol), oleylamine (OAm, 0.7 g), oleic aicd (OA, 0.7 g), and 1-octadecene (7.89 g) was stirred and degassed at 80 °C in an argon atmosphere. The mixture was heated up to 120 °C and was kept at this temperature for 1 minute before $Fe(CO)_5$ (0.07 mL) was injected into the solution. Subsequently, the temperature was raised to 220 °C and kept at this temperature for 20 minutes. The mixture was then heated to 300 °C within 8 minutes and maintained at this temperature for 10 minutes before cooled down to room temperature. The product was washed with ethanol and dispersed in hexane for further use.

Synthesis of FePt-Fe_3O_4/MgO and fct-FePt/MgO NPs: A mixture of magnesium(II) acetylacetonate hydrate ($Mg(acac)_2{\cdot}2H_2O$, 650 mg), OAm (6 mL), OA (1.5 mL), and dibenzyl ether (20 mL) was dissolved under vigorously stirring and degassed at 120 °C in Ar. The as-synthesized FePt/Fe_3O_4 NPs dispersed in 5 mL of hexane was quickly injected into the flask. After hexane was evaporated, the solution was heated up to 300 °C and maintained at this temperature for 60 minutes before it was cooled down to room temperature. The product was washed with ethanol, dried, and then annealed at 700 °C in Ar containing 5 % H_2 for 6 h to obtain fct-FePt/MgO NPs.

Synthesis of fct-FePt NPs: To prepare fct-FePt NPs, 20 mg of FePt/MgO was dissolved in 20 mL ethanol under ultrasonication, and 0.6 mL of concentrated HNO_3 was then added dropwise into the dispersion. The solution was kept under ultrasonication for 5 minutes, followed by centrifugation to separate fct-FePt NPs. The NPs were washed with ethanol twice and dissolved in hexane in the presence of OA and OAm.

Synthesis of 8/4 nm fct-FePt/Co NPs: In a four-neck flask, a mixture of Co^{II} acetylacetonate ($Co(acac)_2$, 40 mg) and OAm (10 mL) was degassed at 120 °C in Ar containing 5 % H_2. 8 mg of fct-FePt NPs in 5 mL hexane was quickly injected into the flask. After hexane was evaporated, the solution was heated up to 320 °C and maintained at this temperature for 60 minutes before it was cooled down to room temperature. The product was collected by an external magnet, washed with ethanol, and dispersed in hexane. To prepare 8/4 nm FePt/Fe_2C core/shell NPs, the precursor was changed to iron(III) acetylacetonate ($Fe(acac)_3$, 40 mg) and the solution was kept at 320 °C for 60 minutes. To prepare 8/4 nm FePt/Ni core/shell NPs, nickel(II) acetylacetonate ($Ni(acac)_2$, 40 mg) was used as precursor and the solution was kept at 200 °C for 30 minutes.

Received: November 8, 2013
Revised: December 7, 2013
Published online: January 21, 2014

Keywords: exchange interactions · intermetallic phases · magnetic properties · nanostructures · reduction

[1] a) O. Gutfleisch, M. A. Willard, E. Bruck, C. H. Chen, S. G. Sankar, J. P. Liu, *Adv. Mater.* **2011**, *23*, 821 – 842; b) R. Skomski, P. Manchanda, P. Kumar, B. Balamurugan, A. Kashyap, D. J. Sellmyer, *IEEE Trans. Magn.* **2013**, *49*, 3215 – 3220; c) N. Poudyal, J. P. Liu, *J. Phys. D* **2013**, *46*; d) R. Skomski, *J. Phys. Condens. Matter* **2003**, *15*, R841 – R896; e) J. M. D. Coey, *Scripta Mater.* **2012**, *67*, 524 – 529.

[2] E. F. Kneller, R. Hawig, *IEEE Trans. Magn.* **1991**, *27*, 3588 – 3600.

[3] R. Skomski, J. M. D. Coey, *Phys. Rev. B* **1993**, *48*, 15812 – 15816.

[4] R. Skomski, J. M. D. Coey, *IEEE Trans. Magn.* **1994**, *30*, 607 – 609.

[5] a) Q. Song, Z. J. Zhang, *J. Am. Chem. Soc.* **2012**, *134*, 10182 – 10190; b) S.-h. Noh, W. Na, J. T. Jang, J. H. Lee, E. J. Lee, S. H. Moon, Y. Lim, J. S. Shin, J. Cheon, *Nano Lett.* **2012**, *12*, 3716 – 3721; c) J. H. Lee, J. T. Jang, J. S. Choi, S. H. Moon, S. H. Noh, J. W. Kim, J. G. Kim, I. S. Kim, K. I. Park, J. Cheon, *Nat. Nanotechnol.* **2011**, *6*, 418 – 422.

[6] a) G. Salazar-Alvarez, H. Lidbaum, A. López-Ortega, M. Estrader, K. Leifer, J. Sort, S. Suriñach, M. D. Baró, J. Nogués, *J. Am. Chem. Soc.* **2011**, *133*, 16738 – 16741; b) X. Sun, N. Frey Huls, A. Sigdel, S. Sun, *Nano Lett.* **2011**, *11*, 246 – 251.

[7] a) S. Sun, *Adv. Mater.* **2006**, *18*, 393 – 403; b) S. H. Sun, C. B. Murray, D. Weller, L. Folks, A. Moser, *Science* **2000**, *287*, 1989 – 1992.

[8] H. Zeng, J. Li, J. P. Liu, Z. L. Wang, S. H. Sun, *Nature* **2002**, *420*, 395 – 398.

[9] H. Zeng, J. Li, Z. L. Wang, J. P. Liu, S. H. Sun, *Nano Lett.* **2004**, *4*, 187 – 190.

[10] N. Sakuma, T. Ohshima, T. Shoji, Y. Suzuki, R. Sato, A. Wachi, A. Kato, Y. Kawai, A. Manabe, T. Teranishi, *ACS Nano* **2011**, *5*, 2806 – 2814.

[11] H. Zeng, S. Sun, J. Li, Z. L. Wang, J. P. Liu, *Appl. Phys. Lett.* **2004**, *85*, 792 – 794.

[12] T. Teranishi, A. Wachi, M. Kanehara, T. Shoji, N. Sakuma, M. Nakaya, *J. Am. Chem. Soc.* **2008**, *130*, 4210 – 4211.
[13] X. Teng, D. Black, N. J. Watkins, Y. Gao, H. Yang, *Nano Lett.* **2003**, *3*, 261 – 264.
[14] X. Liu, S. He, J.-M. Qiu, J.-P. Wang, *Appl. Phys. Lett.* **2011**, *98*, 222507.
[15] J. Chen, X. Ye, S. J. Oh, J. M. Kikkawa, C. R. Kagan, C. B. Murray, *ACS Nano* **2012**, *7*, 1478 – 1486.
[16] J. Kim, C. Rong, Y. Lee, J. P. Liu, S. Sun, *Chem. Mater.* **2008**, *20*, 7242 – 7245.
[17] A. Figuerola, A. Fiore, R. Di Corato, A. Falqui, C. Giannini, E. Micotti, A. Lascialfari, M. Corti, R. Cingolani, T. Pellegrino, P. D. Cozzoli, L. Manna, *J. Am. Chem. Soc.* **2008**, *130*, 1477 – 1487.
[18] J. Kim, C. Rong, J. P. Liu, S. Sun, *Adv. Mater.* **2009**, *21*, 906 – 909.
[19] H. Zeng, S. Sun, *Adv. Funct. Mater.* **2008**, *18*, 391 – 400.
[20] D. Weller, A. Moser, L. Folks, M. E. Best, W. Lee, M. F. Toney, M. Schwickert, J. U. Thiele, M. F. Doerner, *IEEE Trans. Magn.* **2000**, *36*, 10 – 15.

